

Properties of Hot Nuclear Matter

Omar Benhar ¹, Alessandro Lovato ^{2,3}, and Lucas Tonetto ⁴

¹ INFN, Sezione di Roma, 00185 Roma, Italy; omar.benhar@roma1.infn.it

² Physics Division, Argonne National Laboratory, Argonne, Illinois 60439, USA; lovato@alcf.anl.gov

³ INFN, Trento Institute of Fundamental Physics and Applications, 38123 Trento, Italy

⁴ Dipartimento di Fisica, Sapienza Università di Roma, 00185 Roma, Italy; lucas.tonetto@uniroma1.it

Abstract: A fully quantitative description of equilibrium and dynamical properties of hot nuclear matter will be needed for the interpretation of the available and forthcoming astrophysical data, providing information on the post merger phase of a neutron star coalescence. We discuss the results of a recently developed theoretical model, based on a phenomenological nuclear Hamiltonian including two- and three-nucleon potentials, to study the temperature dependence of average and single-particle properties of nuclear matter relevant to astrophysical applications. The potential of the proposed approach for describing dissipative processes leading to the appearance of bulk viscosity in neutron star matter is also outlined.

Keywords: nuclear matter; thermal effects; bulk viscosity; neutron stars.

1. Introduction

The interpretation of the presently available and future astronomical data providing information on the post merger phase of coalescing binary neutron stars will require an accurate description of the properties of dense nuclear matter at temperatures as high as 100 MeV [1–5]. Of great importance, in this context, will be the development of a consistent framework suitable for modelling both the equilibrium configurations—determining the equation of state (EOS) of neutron star matter—and dissipative processes, involving mechanisms that lead to the appearance of bulk viscosity [6] and neutrino emission [7].

The EOS of hot nuclear matter is often derived from dynamical models based on the independent-particle approximation, using Skyrme-type effective interactions [8] or the formalism of quantum field theory and the relativistic mean field (RMF) approximation [9]. More comprehensive studies have been performed within the framework of Nuclear Many-Body Theory, in which the description of nuclear dynamics is based on a phenomenological Hamiltonian strongly constrained by the observed properties of the two- and three-nucleon systems. Calculations along this line have been carried out using both G -matrix perturbation theory and the variational approach based on the formalism of correlated wave functions and the cluster expansion technique; see, e.g., Refs. [10] and [11].

The authors of Refs. [12] have developed a procedure to renormalise the coordinate-space nuclear Hamiltonian by introducing screening effects arising from short-range nucleon-nucleon correlations. The resulting density-dependent effective potential—which includes the contributions of both two- and three-nucleon forces—is well-behaved, and can be employed to carry out perturbative calculations in the basis of eigenstates of the non interacting system. The extension of this formalism to the case of non-zero temperature—involving a proper definition of the grand canonical potential needed to achieve thermodynamic consistency—is based on the assumption that at temperature $T \ll m_\pi$, $m_\pi \approx 150$ MeV being the mass of the π -meson, thermal effects do not significantly affect strong-interaction dynamics [13].

In this paper, we discuss the main features of the approach of Refs. [12,13], as well as its application to a variety of equilibrium and dynamical properties of nuclear matter [14]. The nuclear Hamiltonian and the derivation of the effective interaction are described in

arXiv:2306.01351v1 [nucl-th] 2 Jun 2023

Citation: Benhar, O.; Lovato, A.; Tonetto, L. Properties of Hot Nuclear Matter. *Universe* **2023**, *1*, 0. <https://doi.org/>

Received:

Revised:

Accepted:

Published:

Copyright: © 2023 by the authors. Submitted to *Universe* for possible open access publication under the terms and conditions of the Creative Commons Attribution (CC BY) license (<https://creativecommons.org/licenses/by/4.0/>).

Section 2, while the perturbative calculation of the nuclear matter EOS at finite temperature is outlined in Section 3. Thermal effects on the single-particle properties of charge-neutral β -stable matter are discussed in Sections 5. Finally, Section 6 is devoted to the calculation of the bulk viscosity coefficient, driving the damping of density oscillations of neutron stars.

2. Nuclear Hamiltonian

Nuclear Many-Body Theory (NMBT) is based on the hypothesis that all nucleon systems—from the deuteron to neutron stars—can be described in terms of point like protons and neutrons, the dynamics of which are dictated by the Hamiltonian

$$H = \sum_i \frac{p_i^2}{2m} + \sum_{i<j} v_{ij} + \sum_{i<j<k} V_{ijk}, \quad (1)$$

with m and \mathbf{p}_i being the mass and momentum of the i -th particle.¹

Nucleon-nucleon (NN) potentials that are local or semi-local in coordinate space are usually written in the form

$$v_{ij} = \sum_p v^p(r_{ij}) O_{ij}^p, \quad (2)$$

where $r_{ij} = |\mathbf{r}_i - \mathbf{r}_j|$ is the distance between the interacting particles. They are designed to reproduce the measured properties of the two-nucleon system, in both bound and scattering states, and reduce to the Yukawa one-pion exchange potential at large distances. The sum in Eq. (2) includes up to eighteen terms, with the corresponding operators, O^p , being required to describe the strong spin-isospin dependence and non central nature of nuclear forces ($i = 1, \dots, 6$), as well as the occurrence of spin-orbit and other angular-momentum dependent interactions ($i = 7, \dots, 14$). Highly accurate phenomenological potentials, such as the Argonne v_{18} (AV18) model, also feature additional terms accounting for small violations of charge symmetry and charge independence ($i = 15, \dots, 18$) [15].

The addition of the three-nucleon (NNN) potential V_{ijk} is needed to model the effects of *irreducible* three-body interactions, reflecting the appearance of processes involving the internal structure of the nucleons. Nuclear Hamiltonians comprising the AV18 NN potential and a phenomenological NNN potential designed to explain the binding energies of ${}^3\text{He}$ and ${}^4\text{He}$ and the empirical equilibrium density of isospin-symmetric matter—such as the widely used Urbana IX (UIX) model [16,17]—have been shown to possess a remarkable predictive power. The results of Quantum Monte Carlo (QMC) calculations, extensively reviewed in Ref.[18], demonstrate that the AV18 + UIX Hamiltonian is capable describe the energies of the ground and low-lying excited states of nuclei with mass number $A \leq 8$ to few percent accuracy.

2.1. Renormalisation of the nucleon-nucleon interaction

Owing to the presence of a strong repulsive core, the matrix elements of the NN potential between eigenstates of the non interacting system are large, and standard perturbation theory cannot be used to carry out calculations of nuclear-matter properties.

The renormalisation scheme based on the formalism of correlated basis functions (CBF) and the cluster expansion technique [19,20] allows one to determine an effective interaction suitable to carry out perturbative calculations in coordinate space. This approach, originally proposed by Cowell and Pandharipande in the early 2000s [21,22] and further developed by the authors of Refs. [23–25], has been extensively employed to study nuclear matter and neutron stars [12–14]. The resulting potential, can be written as in Eq. (2) including terms with $i \leq 6$, associated with the operators

$$O_{ij}^{p \leq 6} = [1, (\boldsymbol{\sigma}_i \cdot \boldsymbol{\sigma}_j), S_{ij}] \otimes [1, (\boldsymbol{\tau}_i \cdot \boldsymbol{\tau}_j)]. \quad (3)$$

¹ In this article, we adopt the system of natural units, in which $\hbar = c = k_B = 1$, and, unless otherwise specified, neglect the small proton-neutron mass difference.

Here σ_i and τ_i are Pauli matrices acting in spin and isospin space, respectively, while the angular dependence is described by the tensor operator S_{ij} , defined as

$$S_{ij} = \frac{3}{r_{ij}^2} (\sigma_i \cdot \mathbf{r}_{ij})(\sigma_j \cdot \mathbf{r}_{ij}) - (\sigma_i \cdot \sigma_j). \quad (4)$$

Note that the OPE potential can also be written in terms of the $O_{ij}^{p \leq 6}$ defined by Eqs.(3) and (4).

The CBF effective interaction is *defined* by the equation

$$\langle H \rangle = \langle \Psi_0 | H | \Psi_0 \rangle = T_F + \langle \Phi_0 | \sum_{i < j} v_{ij}^{\text{eff}} | \Phi_0 \rangle. \quad (5)$$

where, $|\Phi_0\rangle$ and T_F denote the ground state of the non interacting Fermi gas at density ρ and the corresponding energy, respectively, while H is the nuclear Hamiltonian of Eq. (1). The *correlated* ground state, $|\Psi_0\rangle$, is obtained from the corresponding Fermi gas state $|\Phi_0\rangle$ through the transformation

$$|\Psi_0\rangle \equiv \frac{F|\Phi_0\rangle}{\langle \Phi_0 | F^\dagger F | \Phi_0 \rangle^{1/2}}, \quad (6)$$

where the operator F is a symmetrized product of two-body correlation operators, whose structure is chosen in such a way as to reflect the complexity of NN forces.

The effective interaction employed to obtain the results discussed in this paper has been derived following the procedure described in Ref. [24], which allows to include the contribution of three-nucleon clusters to the ground-state expectation value $\langle H \rangle$ appearing in the left-hand side of Eq. (5). This feature is essential to take into account three-nucleon interactions, which play a dominant role in the high-density regime relevant to astrophysical applications.

2.2. The CBF effective interaction

The nuclear Hamiltonian employed to obtain the CBF effective interaction consists of the Argonne v'_6 (AV6P) NN potential—determined projecting the full AV18 potential onto the operator basis of Eq.(3) [26]—and the UIX NNN potential [17]. The AV6P potential predicts the binding energy and electric quadrupole moment of the deuteron with accuracy of 1%, and 4%, respectively, and provides an excellent fit of the elastic NN scattering phase shifts in the 1S_0 channel—which is dominant in pure neutron matter—up to lab energy ~ 600 MeV, well above pion production threshold..

The UIX potential is written in the form

$$V_{ijk} = V_{ijk}^{2\pi} + V_{ijk}^R, \quad (7)$$

where the first term is the attractive Fujita-Miyazawa potential [27]—describing two-pion exchange NNN interactions with excitation of a Δ -resonance in the intermediate state—while the purely phenomenological V_{ijk}^R is an isoscalar repulsive term, the strength of which is fixed in such a way as to reproduce the saturation density of isospin symmetric matter inferred from nuclear systematics [16,17].

Note that the CBF effective interaction depends on density through both dynamical correlations, described by the operator F of Eq.(6), and statistical correlations, arising from the antisymmetric nature of the state $|\Phi_0\rangle$. The radial dependence of v^{eff} in the $S = 0$ and $T = 1$ channel at baryon density $\rho = 0.04, 0.32$ and 0.48 fm^{-3} is displayed in Fig. 1. The effect of renormalisation clearly emerges from the comparison with the bare AV6P potential.

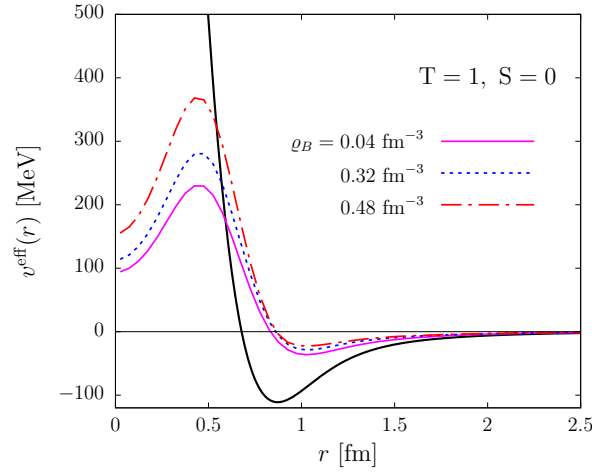


Figure 1. Radial dependence of the CBF effective potential in the $S = 0, T = 1$ channel. The solid, dashed, and dot-dash lines correspond to baryon number density $\rho = 0.04, 0.32$ and 0.48 fm^{-3} . For comparison, the thick solid line shows the bare AV6P potential.

Recent studies of the EOS of cold neutron matter—performed by the authors of Ref. [28] using accurate computational techniques—show that the predictions of the somewhat simplified AV6P + UIX Hamiltonian are very close to those obtained from the full AV18 + UIX model employed by Akmal, Pandharipande and Ravenhall [29].

3. Many-Body Perturbation Theory at Finite Temperature

Let us consider, for simplicity, a one-component Fermi system. The derivation of perturbation theory at finite-temperature is based on the solution of the Bloch equation

$$-\frac{\partial \Phi}{\partial \beta} = (H - \mu N)\Phi, \quad (8)$$

where

$$\Phi(\beta) = e^{-\beta(H - \mu N)}, \quad (9)$$

with the initial condition $\Phi(0) = 1$; see, e.g., Ref. [30]. In the above equations $\beta = 1/T$, while H and μ denote the Hamiltonian and the chemical potential, respectively.

The perturbative expansion of the grand canonical partition function $Z = \text{Tr } \Phi$ is easily obtained exploiting the formal similarity between Eq. (8) and the time-dependent Schrödinger equation of quantum mechanics, and rewriting the Hamiltonian in the form

$$H = H_0 + H_I. \quad (10)$$

Substitution of Eq. (10) into the right-hand side of the Bloch equation, leading to

$$-\frac{\partial \Phi}{\partial \beta} = [(H_0 - \mu N) + H_I]\Phi = (H'_0 + H_I)\Phi,$$

shows that the formalism of time-dependent perturbation theory can be readily generalised by replacing $t \rightarrow -i\beta$, and using H'_0 to define operators in the interaction picture.

The fundamental relation

$$\Omega = -\frac{1}{\beta} \ln Z = -PV = F - \mu N = E - TS - \mu N, \quad (11)$$

where V is the normalization volume, provides the link between the grand canonical potential Ω , the pressure P , and the free energy $F = E - TS$, with E and S being the energy and entropy of the system, respectively; see, e.g., Ref. [31]. From Eq. (11) it follows that

$$P = -\frac{\Omega}{V}, \quad S = -\frac{\partial \Omega}{\partial T}, \quad N = -\frac{\partial \Omega}{\partial \mu}. \quad (12)$$

In the following, we will discuss the application of the above results to a system described by the Hamiltonian (10), with

$$H_0 = \sum_k e_k a_k^\dagger a_k, \quad (13)$$

where, in general

$$e_k = \frac{\mathbf{k}^2}{2m} + U_k = t_k + U_k, \quad (14)$$

and

$$H_I = \sum_{k,k',q,q'} \langle k'q' | v | kq \rangle a_{k'}^\dagger a_q^\dagger a_q a_k - \sum_k U_k a_k^\dagger a_k. \quad (15)$$

Here, the label k specifies both the particle momentum and the discrete quantum numbers corresponding to one-particle states, a_k^\dagger and a_k denote creation and annihilation operators, respectively, and v is the potential describing interparticle interactions. The single-particle potential U_k , which in principle does not affect the results of calculations of physical quantities, is chosen in such a way as to improve the convergence of the perturbative expansion, or fulfil specific conditions; see, e.g., Ref. [32].

It has to be pointed out that, according to Eq. (11), the pressure can be written in the form

$$P = \varrho \left(\mu - \frac{F}{N} \right), \quad (16)$$

with $\varrho = N/V$, implying that at equilibrium, that is, for $P = 0$, $\mu = F/N$. This result is the generalisation of the Hugenholtz-Van Hove theorem [33] to the case of non vanishing temperature.

It should be emphasised that, when used in conjunction with the CBF effective interaction discussed in Section 2.2, the perturbative approach based on the Hamiltonian defined by Eqs. (10) and (13)-(15) allows to take into account two- and three-nucleon interactions in a fully consistent fashion.

3.1. Perturbative expansion

At first order in H_I , the grand canonical potential is given by [34]

$$\Omega = \Omega_0 + \Omega_1, \quad (17)$$

with

$$\Omega_0 = -\frac{1}{\beta} \sum_k \ln \{ 1 + e^{-[\beta(e_k - \mu)]} \}, \quad (18)$$

$$\Omega_1 = \frac{1}{2} \sum_{kk'} \langle kk' | v | kk' \rangle_A n_k n_{k'} - \sum_k U_k n_k, \quad (19)$$

where $|kk'\rangle_A = |kk'\rangle - |k'k\rangle$ denotes an antisymmetrised two-particle state, and n_k is the Fermi distribution, defined as

$$n_k = [1 + e^{\beta(e_k - \mu)}]^{-1}. \quad (20)$$

From Eqs. (18) and (19) it follows that the free energy per particle

$$\frac{F}{N} = \frac{1}{N}(\Omega_0 + \Omega_1) + \mu, \quad (21)$$

can be cast in the form

$$\begin{aligned} \frac{F}{N} = \frac{1}{N} \left\{ \sum_k t_k n_k + \frac{1}{2} \sum_{k,k'} \langle kk' | v | kk' \rangle_A n_k n_{k'} \right. \\ \left. + \frac{1}{\beta} \sum_k [n_k \ln n_k + (1 - n_k) \ln(1 - n_k)] + \mu \left(1 - \frac{1}{N} \sum_k n_k \right) \right\}. \end{aligned} \quad (22)$$

In principle, for any assigned values of temperature and chemical potential, the above equations provide a scheme for the determination of the equation of state of nuclear matter at finite temperature, $P = P(\mu, T)$. Because baryon number is conserved by all known interactions, however, in nuclear matter it is more convenient to use baryon density as an independent variable, and determine the chemical potential from the relation

$$\varrho = -\frac{1}{V} \frac{\partial}{\partial \mu} (\Omega_0 + \Omega_1). \quad (23)$$

In the $T \rightarrow 0$ limit the momentum distribution reduces to the Heaviside step function $\theta(\mu - e_k)$, and the chemical potential is given by $\mu = e_{k_F}$, with the Fermi momentum defined as $k_F = (6\pi^2 \varrho / v)^{1/3}$.

3.2. Thermodynamic consistency

For $T \neq 0$ and density-dependent potentials, thermodynamic consistency is not trivially achieved at any given order of perturbation theory. A clear manifestation of this difficulty is the mismatch between the value of pressure obtained from Eq. (16) and the one resulting from the alternative—although in principle equivalent—thermodynamic expression

$$P = -\frac{\partial F}{\partial V} = \varrho^2 \frac{\partial F}{\partial \varrho} \frac{1}{N}. \quad (24)$$

A procedure fulfilling the requirement of thermodynamic consistency by construction can be derived from a variational approach, based on minimisation of the trial grand canonical potential [35]

$$\begin{aligned} \tilde{\Omega} = \sum_k t_k n_k + \frac{1}{2} \sum_{k,k'} \langle kk' | v | kk' \rangle_A n_k n_{k'} \\ + \frac{1}{\beta} \sum_k [n_k \ln n_k + (1 - n_k) \ln(1 - n_k)], \end{aligned} \quad (25)$$

with respect to the form of distribution n_k . Note that the above expression—the use of which is fully legitimate in the variational context—can also be obtained in first order perturbation theory neglecting terms involving $\partial \Omega_1 / \partial T$ and $\partial \Omega_1 / \partial \mu$ [34].

The condition

$$\frac{\delta \tilde{\Omega}}{\delta n_k} = 0, \quad (26)$$

turns out to be satisfied by the distribution function

$$n_k = \{1 + e^{\beta[(t_k + U_k + \delta e) - \mu]}\}^{-1}, \quad (27)$$

with

$$U_k = \sum_{k'} \langle kk' | v | kk' \rangle_A n_{k'}, \quad (28)$$

and

$$\delta e = \frac{1}{2} \sum_{k, k'} \langle kk' | \frac{\partial v}{\partial \rho} | kk' \rangle_A n_k n_{k'}. \quad (29)$$

Within the above scheme, that reduces to the standard Hartee-Fock approximation in the case of density-independent potentials, all thermodynamic functions at given temperature and baryon density can be consistently obtained using the distribution n_k of Eq. (27). Note, however, that, because both U_k and δe depend on n_k , see Eqs. (28) and (29), calculations must be carried out self-consistently, applying an iterative procedure.

4. Equilibrium properties of hot nuclear matter

Consider now a nucleon system at temperature T , baryon number density ρ and proton number density $\rho_p = Y_p \rho$. At first order in the CBF effective interaction v^{eff} , the internal energy per nucleon can be written in the form [14]

$$\frac{E}{N} = \frac{1}{N} \left\{ \sum_{\alpha \mathbf{k}} \frac{\mathbf{k}^2}{2m} n_{\alpha}(k, T) + \frac{1}{2} \sum_{\alpha \mathbf{k}} \sum_{\alpha' \mathbf{k}'} \langle \alpha \mathbf{k}, \alpha' \mathbf{k}' | v^{\text{eff}} | \alpha \mathbf{k}, \alpha' \mathbf{k}' \rangle_A n_{\alpha}(k, T) n_{\alpha'}(k', T) \right\}. \quad (30)$$

In the above equations, the index $\alpha = n, p$ labels neutrons and protons, respectively, \mathbf{k} is the nucleon momentum, $k = |\mathbf{k}|$, and $|\alpha \mathbf{k}, \alpha' \mathbf{k}' \rangle_A$ denotes an antisymmetrised two-nucleon state. Conservation of baryon number obviously implies that $Y_n = 1 - Y_p$.

The temperature dependence is described by the Fermi distributions

$$n_{\alpha}(k, T) = \left\{ 1 + \exp[\beta(e_{\alpha k} - \mu_{\alpha})] \right\}^{-1}. \quad (31)$$

where the single-particle energies are defined as,

$$e_{\alpha k} = e_{\alpha k}^{\text{HF}} + \delta e, \quad (32)$$

with

$$e_{\alpha k}^{\text{HF}} = \frac{\mathbf{k}^2}{2m} + \sum_{\alpha' \mathbf{k}'} \langle \alpha \mathbf{k}, \alpha' \mathbf{k}' | v^{\text{eff}} | \alpha \mathbf{k}, \alpha' \mathbf{k}' \rangle_A n_{\alpha'}(k', T), \quad (33)$$

and

$$\delta e = \frac{\rho}{2} \sum_{\alpha \mathbf{k}} \sum_{\alpha' \mathbf{k}'} \langle \alpha \mathbf{k}, \alpha' \mathbf{k}' | \frac{\partial v^{\text{eff}}}{\partial \rho} | \alpha \mathbf{k}, \alpha' \mathbf{k}' \rangle_A n_{\alpha}(k, T) n_{\alpha'}(k', T), \quad (34)$$

The correction to the Hartree Fock (HF) spectrum is needed to satisfy the requirement of thermodynamic consistence, and vanishes in the case of a density-independent potential [13]. The chemical potentials μ_{α} are determined by the normalisation conditions

$$2 \sum_{\alpha \mathbf{k}} n_{\alpha}(k, T) = N_{\alpha}, \quad (35)$$

where N_α denotes the number of particles of species α , the fractional density of which is $Y_\alpha = N_\alpha/N_B = \rho_\alpha/\rho$. Note that the above definitions imply that both the single-nucleon energies and the chemical potentials depend on temperature through the Fermi distribution.

The free energy per nucleon is obtained from

$$\frac{F}{N} = \frac{1}{N}(E - TS), \quad (36)$$

with the internal energy per nucleon of Eq. (30) and the entropy per nucleon defined as

$$\frac{S}{N} = - \sum_{\alpha \mathbf{k}} \left\{ n_\alpha(k, T) \ln n_\alpha(k, T) + [1 - n_\alpha(k, T)] \ln [1 - n_\alpha(k, T)] \right\}. \quad (37)$$

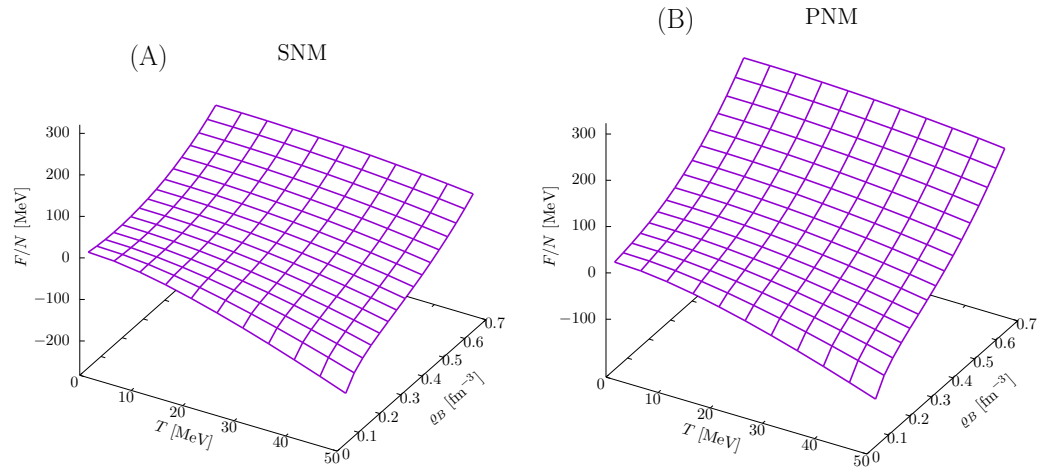


Figure 2. Density and temperature dependence of the free energy per nucleon of SNM (A) and PNM (B), computed using Eqs. (30)-(37), with the CBF effective interaction discussed in Section 2.2.

Figure 2 shows the density and temperature dependence of the free energy per nucleon of isospin-symmetric matter (SNM) and pure neutron matter (PNM), corresponding to proton fraction $Y_p = 0.5$ and 0, respectively, obtained from the procedure described above using the CBF effective interaction.

5. Thermal effects on nuclear matter properties

In the temperature regime discussed in this paper, thermal modifications of nuclear matter properties arise primarily from the Fermi distributions, defined by Eq. (31). Comparison to the $T \rightarrow 0$ limit shows that the probability distribution $n_\alpha(k, T > 0)$ is reduced from unity in the region corresponding to $\mu_\alpha - T \lesssim e_{\alpha k} \lesssim \mu_\alpha$, and acquires non vanishing positive values for $\mu_\alpha \lesssim e_{\alpha k} \lesssim \mu_\alpha + T$. It follows that, for any given temperature T , the extent of thermal modifications to the Fermi distribution is driven by the ratio $2T/\mu_\alpha$. This observation in turn implies that, because the chemical potential is a monotonically increasing function of the particle density ρ_α over a broad range of temperatures, for any given T thermal effects turn out to be more significant at lower ρ_α . On the other hand, they become vanishingly small in the high-density regime, in which degeneracy dominates.

5.1. Charge-neutral β -stable matter at finite temperature

In charge-neutral matter consisting of neutrons, protons and leptons in equilibrium with respect to the weak interaction processes

$$n \rightarrow p + \ell + \bar{\nu}_\ell, \quad p + \ell^- \rightarrow n + \nu_\ell, \quad (38)$$

where $\ell = e, \mu$ labels the lepton flavour, the proton fraction Y_p is uniquely determined by the equations

$$\mu_n - \mu_p = \mu_\ell, \quad Y_p = \sum_\ell Y_\ell. \quad (39)$$

At densities such that the electron chemical potential does not exceed the rest mass of the muon, $m_\mu = 105.7$ MeV, the sum appearing in the above equation includes electrons only. At higher densities—typically at $\rho \gtrsim \rho_0$, with $\rho_0 = 0.16 \text{ fm}^{-3}$ being the baryon number density of isospin-symmetric matter in thermodynamic equilibrium at $T = 0$ —the appearance of muons becomes energetically favoured, and must be taken into account.

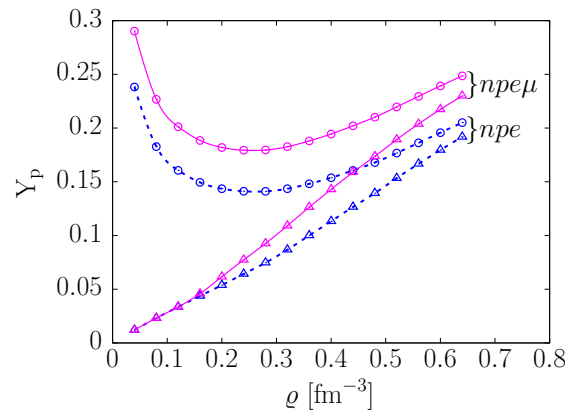


Figure 3. Density dependence of the proton fraction in charge-neutral β -stable matter. Solid lines marked with triangles and circles correspond to $npe\mu$ matter at $T = 0$ and 50 MeV, respectively. The same quantities in npe matter are represented by dashed lines. From Ref. [14].

The solid lines of Fig. 3 show the density dependence of the proton fractions corresponding to β -equilibrium of matter consisting of protons, neutrons, electrons and muons, or $npe\mu$ matter, at $T = 0$ (triangles) and 50 MeV (circles) [14]. The results have been obtained assuming that neutrinos do not interact with matter, and have therefore vanishing chemical potential. For comparison, the same quantities in npe matter, in which the muon contribution is not included, are displayed by the dashed lines. The most prominent thermal effect is a significant departure from the monotonic behaviour observed in cold matter. The emergence of a minimum in the density dependence of the proton fraction results from the balance between the thermal and degeneracy contributions to the chemical potentials appearing in Eq. (39). For $T \gtrsim 20$ MeV and low density, typically $\rho \lesssim \rho_0$, the thermal contribution—whose leading order term can be written in the form $\delta\mu_\alpha \propto T^2/\rho_\alpha^{1/3}$ —turns out to be much larger for protons than for neutrons, and β -equilibrium requires large proton fractions. The results displayed in Fig. 3, showing that Y_p does not exceed 25% for $\rho_0/2 \leq \rho \leq 4\rho_0$, imply that in β -stable matter thermal effects affect mainly the proton distributions.

The description of single-particle dynamics in interacting many-body systems is largely based on the use of the effective mass m_α^* , defined as

$$\frac{1}{m_\alpha^*} = \left(\frac{1}{k} \frac{de_{\alpha k}}{dk} \right)_{k=k_{F_\alpha}}, \quad (40)$$

with $e_{\alpha k}$ given by Eq.(32). The effective mass dictates the nucleon dispersion relation in matter, which plays a critical role in determining the rates of many processes relevant to neutron star properties, such as the bulk viscosity to be discussed in Section 6. The

momentum dependence of the nucleon spectra in cold nuclear matter is often parametrised according to [7]

$$e_{\alpha k} = \frac{k^2}{2m_0^*} + U_\alpha, \quad (41)$$

where m_0^* denotes the value of m_α^* at $T = 0$, while the offset U_α from the free-nucleon spectrum—the value of which depends on *both* temperature and density—is determined by the requirement that the above approximation reproduce the results of the full microscopic calculation at $k = 0$.

The solid lines of Fig. 4 show the momentum dependence of the proton spectra in charge-neutral β -stable matter at baryon density $\rho = 2\rho_0$ and temperature $T = 0$ and 50 MeV. A comparison with the dashed lines indicates that at $T = 50$ MeV the approximation of Eq. (41) fails to provide an accurate representation of $e_{\alpha k}$ for $k > 0.5 \text{ fm}^{-1}$. However, the quadratic approximation turns out to be in remarkable agreement with the microscopic result if m_0^* is replaced with the effective mass computed at $T = 50$ MeV.

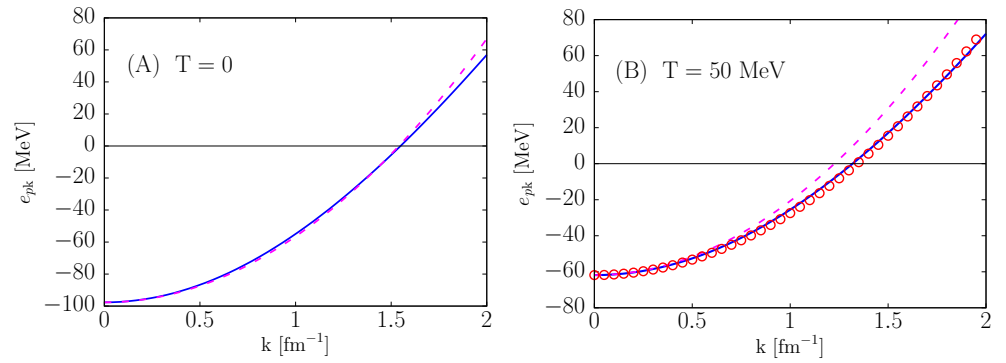


Figure 4. Momentum dependence of the proton spectrum in charge-neutral β -stable matter at baryon density $\rho = 2\rho_0$ and temperature $T = 0$ (A) and 50 MeV (B). The solid and dashed lines represent the result of full microscopic calculations and the approximation of Eq. (41), respectively. The open circles in panel (B) have been obtained using the quadratic approximation with m_0^* replaced by the effective mass computed at $T = 50$ MeV.

6. Bulk viscosity of neutron star matter

Bulk viscosity in charge-neutral β -stable matter appears in the aftermath of an instantaneous departure from β -equilibrium, resulting from the change of density and pressure induced by some perturbation. The role of bulk viscosity in determining the maximum rotation rate of neutron stars—the value of which is limited by the onset of the Chandrasekhar-Friedman-Shutz (CFS) instability, driven by gravitational wave emission [36–38]—has been discussed by many authors; for a review, see, e.g., Ref. [39]. More recent studies, motivated by the observation of the gravitational wave event GW170817 [40], focused on the effect of bulk viscosity in neutron star mergers, leading to a damping of density oscillations [41].

6.1. Dissipative processes in fluids

The description of fluids is based on the continuity equation expressing conservation of mass

$$\frac{\partial \rho}{\partial t} = -\nabla \cdot (\rho \mathbf{v}), \quad (42)$$

where $\mathbf{v} = \mathbf{v}(\mathbf{r}, t)$ and $\varrho = \varrho(\mathbf{r}, t)$ denote the velocity field and matter density, respectively. For ideal fluids, that is, in the absence of dissipation, the force acting on a fluid element is simply related to the pressure of the surrounding medium through

$$\mathbf{F} = -\nabla P, \quad (43)$$

and the equation of motion reduces to Euler's equation [42]

$$\frac{\partial \mathbf{v}}{\partial t} + (\mathbf{v} \cdot \nabla) \mathbf{v} = -\frac{1}{\varrho} \nabla P. \quad (44)$$

The above equations can be combined to obtain

$$\frac{\partial(\varrho \mathbf{v}_i)}{\partial t} = -\nabla_j \Pi_{ij}, \quad (45)$$

where a sum on the index j is implicit and Π_{ij} is the momentum flux tensor, defined as

$$\Pi_{ij} = P\delta_{ij} + \varrho v_i v_j. \quad (46)$$

In viscous fluids, the form of the continuity equation does not change, but the momentum flux tensor needs to be modified by adding a term describing the deviations from the ideal fluid behaviour, due the occurrence of processes involving *irreversible* momentum transfer. The resulting expression can be written in the form

$$\Pi_{ij} = P\delta_{ij} + \varrho v_i v_j + \delta \Pi_{ij}, \quad (47)$$

where

$$\delta \Pi_{ij} = -\eta \left[\nabla_j v_i + \nabla_i v_j + \frac{2}{3} \delta_{ij} (\nabla \cdot \mathbf{v}) \right] - \zeta \delta_{ij} (\nabla \cdot \mathbf{v}), \quad (48)$$

with the two velocity-independent quantities η and ζ being referred to as shear and bulk viscosity coefficients, respectively. In the case of incompressible fluids, in which ϱ does not depend on either \mathbf{r} or t , Eq. (42) implies

$$\nabla \cdot \mathbf{v} = 0, \quad (49)$$

and the contribution of bulk viscosity vanishes.

A pulsation of frequency ω induces a variation of the fluid density described by the equation

$$\varrho(t) = \varrho_{\text{eq}} + \delta \varrho \cos \omega t, \quad (50)$$

where ϱ_{eq} is the density corresponding to chemical equilibrium and $(\delta \varrho / \varrho_{\text{eq}}) \ll 1$. The rate of energy-density dissipation due to bulk viscosity, averaged over the pulsation period $\tau = 2\pi/\omega$, is given by [43]

$$\left\langle \frac{d\epsilon_{\text{diss}}}{dt} \right\rangle = -\frac{1}{\tau} \int_0^\tau dt \nabla_i [-v_j \zeta \delta_{ij} (\nabla \cdot \mathbf{v})] = \frac{1}{\tau} \int_0^\tau dt \zeta (\nabla \cdot \mathbf{v})^2. \quad (51)$$

6.2. Bulk viscosity of β -stable matter

The authors of refs. [44,45] have derived the expression of the bulk viscosity coefficient of β -stable matter under the assumption that neutrinos and antineutrinos are produced through the processes

$$p + e \rightarrow n + \nu_e, \quad (52)$$

$$n \rightarrow p + e + \bar{\nu}_e, \quad (53)$$

referred to as *direct* Urca reactions. They followed the scheme originally proposed in Ref. [46], and employed a simple parametrisation of the nuclear matter EOS assuming a quadratic dependence on the neutron excess $\alpha = 1 - 2Y_p$.

Bulk viscosity is associated with deviations from beta equilibrium, signaled by a non vanishing difference between the neutrino and antineutrino production rates

$$\Delta\Gamma = \Gamma_{\nu_e} - \Gamma_{\bar{\nu}_e}, \quad (54)$$

with $\Delta\Gamma$ being a function of the variable $\delta\mu$, describing the departure from chemical equilibrium. In the case of non degenerate neutrinos

$$\delta\mu = \mu_n - \mu_p - \mu_e. \quad (55)$$

Under the assumption that $\delta\mu \ll T \ll \mu_i$, $\Delta\Gamma$ can be expanded in powers of $\delta\mu$. At leading order one finds

$$\Delta\Gamma = \lambda\delta\mu, \quad (56)$$

with

$$\lambda = 2 \left(\frac{\partial \Gamma_\nu}{\partial \delta\mu} \right)_{\delta\mu=0}. \quad (57)$$

The energy-density dissipation rate—averaged over the period of the density fluctuation of Eq. (50)—can be written in terms of the change of pressure associated with the departure from chemical equilibrium using

$$\begin{aligned} \left\langle \frac{d\epsilon_{\text{diss}}}{dt} \right\rangle &= \frac{1}{\rho} \frac{1}{\tau} \int_0^\tau dt \delta P_{\text{chem}} \frac{d\rho}{dt} \\ &= \frac{\delta\rho}{\rho} \frac{\omega}{\tau} \int_0^\tau dt \delta P_{\text{chem}} \sin \omega t, \end{aligned} \quad (58)$$

with [46]

$$\delta P_{\text{chem}} = -\lambda C^2 \frac{\delta\rho}{\rho} \frac{\omega}{\omega^2 + (2\lambda B/\rho)^2} \sin \omega t + \dots \quad (59)$$

where the ellipses refer to additional terms giving vanishing contributions to the integral. Here, λ is given by Eq. (57), and the constants B and C are defined as

$$B = \left(\frac{\partial \delta\mu}{\partial \alpha} \right)_{\delta\rho=0}, \quad C = \left[\rho \left(\frac{\partial \delta\mu}{\partial \rho} \right) \right]_{\alpha=\alpha_{\text{eq}}}, \quad (60)$$

where α_{eq} is the value of neutron excess corresponding to β -equilibrium. Substitution of Eq. (59) into Eq. (58) yields

$$\left\langle \frac{d\epsilon_{\text{diss}}}{dt} \right\rangle = -\lambda \frac{\omega^2}{2} \left(\frac{\delta\rho}{\rho} \right)^2 \frac{C^2}{\omega^2 + (2B\lambda/\rho)^2}.$$

The bulk viscosity coefficient is obtained combining the above equation with Eqs. (51), which can be rewritten using the continuity equation associated with conservation of baryon number, implying

$$\nabla \cdot \mathbf{v} = -\frac{1}{\rho} \frac{\partial \rho}{\partial t} = \omega \frac{\delta\rho}{\rho} \sin \omega t. \quad (61)$$

Following this procedure, one finally arrives at

$$\zeta = -\lambda \frac{C^2}{\omega^2 + (2B\lambda/\varrho)^2}. \quad (62)$$

The above result shows that the calculation of the bulk viscosity coefficient involves λ , which is obtained from the neutrino and antineutrino production rates, and the constants B and C defined by Eqs. (60). We have studied the density and temperature dependence of ζ using the nuclear matter model described in the previous sections, which allows to take into account thermal modifications of the chemical potentials and effective masses within a fully consistent framework.

6.3. Calculation of the bulk viscosity coefficient

The calculations of the rates of neutrino and antineutrino production in the Urca processes of Eqs. (52) and (53)—needed to obtain λ from Eq. (57)—have been performed using an *improved* version of the commonly used Fermi surface approximation. The important new feature of this procedure lies in the fact that the effective masses depend on temperature, and so does the phase space integration.

Equation (62) can be written in a somewhat more transparent form in terms of the equilibration rate $\gamma = -2B\lambda/\varrho$. The resulting expression

$$\zeta = \varrho \frac{C^2}{B} \frac{1}{2} \frac{\gamma}{\omega^2 + \gamma^2}, \quad (63)$$

exhibits a resonant maximum located at $\gamma = \omega$. This property, which depends on both density and temperature, has been thoroughly analysed by the authors of Ref. [41], who also discussed the differences between the isothermal and adiabatic treatment of thermodynamic quantities.

Under the assumption that during a neutron star merger the heat flow between adjoining fluid elements be negligible, the derivatives involved in the calculations of the quantities B and C defined by Eq. (60) must be computed keeping the entropy per baryon constant. The alternative procedure based on isothermal derivation, while being equivalent in the $T \rightarrow 0$ limit, leads to sizeably different results in the high-temperature regime.

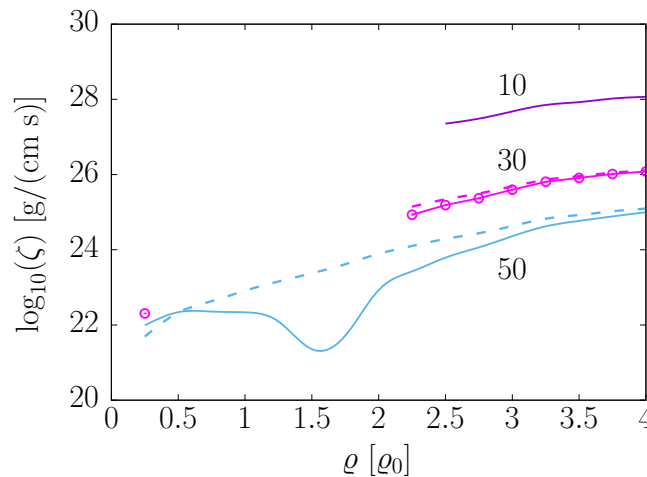


Figure 5. Density dependence of the bulk viscosity coefficient of β -stable matter associated with a density fluctuation of frequency $\omega = 2\pi \times 1$ kHz. The results have been obtained by performing the derivatives of Eqs. (60) using both the isothermal (solid lines and open circles) and adiabatic (dashed lines) definitions. The labels specify the temperature in units of MeV.

Figure 5 shows the behaviour of ζ as a function of density for temperatures 10, 30, and 50 MeV, with the frequency of the density oscillation driving the appearance of viscosity

being set to $\omega = 2\pi \times 1$ kHz, a value typical of neutron star pulsations. The results have been obtained by performing the derivatives of Eqs. (60) using both the isothermal (solid lines and open circles) and adiabatic (dashed lines) definitions.

The peculiar density dependence featured by the solid line corresponding to the highest temperature, $T = 50$ MeV, results from the occurrence of a minimum in the proton fraction $Y_p(\rho)$ —clearly visible in Fig. 3—and from the fact that the value of Y_p exceeds the threshold for the onset of direct Urca processes at all densities. A comparison to the corresponding dashed line shows that the minimum of $\zeta(\rho)$ is entirely washed out when the isothermal derivative is replaced by the adiabatic one. Because the proton fraction is still above the Urca threshold, however, one finds $\zeta(\rho) \neq 0$ over the whole density range of the figure.

A similar pattern is displayed by the solid line and the open circles representing the results obtained at $T = 30$ MeV, although in this case the minimum of $Y_p(\rho)$ is not reflected by a minimum in $\zeta(\rho)$. One only observes an isolated point with $\zeta \neq 0$ located at $\rho = 0.25 \rho_0$, and a density region extending up to $\rho > 2.25 \rho_0$ in which $\zeta = 0$. At larger densities, Y_p is always above the threshold of Urca processes, and $\zeta \neq 0$. At $T = 10$ MeV the solid and dashed lines turn out to lie on top of one another.

It should be noted that, although at high temperatures the Urca process is always allowed, the corresponding values of ζ are very small, and bulk viscosity is unlikely to be distinguished from other dissipative phenomena active in a neutron-star merger.

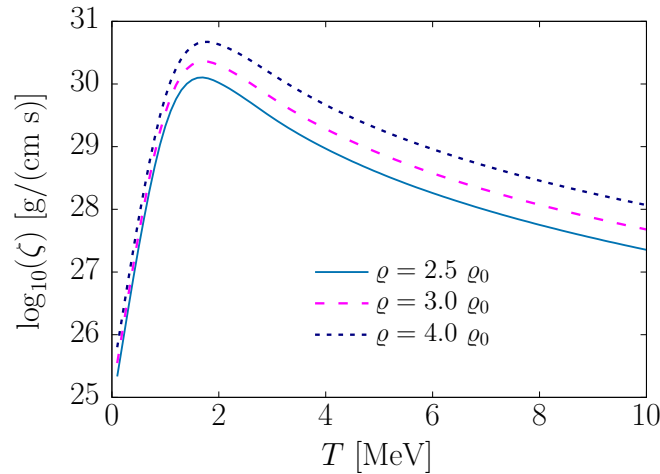


Figure 6. Temperature dependence of the bulk viscosity coefficient ζ corresponding to $\omega = 2\pi \times 1$ kHz and different densities.

The temperature-dependence of the bulk viscosity coefficient at $\omega = 2\pi \times 1$ kHz and densities $\rho = 2.5, 3,$ and $4 \rho_0$ is illustrated in Fig. 6. The maximum at $T \approx 2$ MeV, whose value monotonically increases with density, is clearly apparent. Owing to the low-temperature range spanned by the figure, in this instance the results obtained using isothermal and adiabatic derivatives turn out to be nearly identical. For this reason, only isothermal results are shown.

7. Discussion

The description of neutron-star mergers, which will be needed for the interpretation of current and future astronomical observations, requires a quantitative understanding of both equilibrium and dynamical properties of hot and dense matter. In this context, the availability of a dynamical model strongly constrained by phenomenology and suitable for use in finite-temperature perturbation theory will be crucial.

The approach described in this paper has been employed to obtain the EOS of matter with arbitrary neutron excess in the density region extending up to $4 \rho_0$ —in which the applicability of the description in terms of nucleons is supported by electron-nucleus

scattering data [47]—and temperatures up to 50 MeV. Single-nucleon properties, such as the quasiparticle spectra and effective masses, have been also computed within a theoretical framework in which thermal effects are consistently taken into account. Exploratory studies of dissipative processes leading to the damping of density oscillations in neutron-star mergers suggest that a detailed treatment of thermal effects is needed to clarify important issues, such as the onset of the Urca process.

The extension of the approach outlined in this paper to the description of neutrino emission processes and the neutrino mean free path along the line described in Refs. [24,25] does not involve any conceptual issues, and is currently under way.

Author Contributions: All authors contributed to conceptualisation, development of the formalism and the computing codes, and manuscript preparation. All authors have read and agreed to the published version of the manuscript.

Funding: This research was funded by the U.S. Department of Energy, Office of Science, Office of Nuclear Physics, under contract DE-AC02-06CH11357 (A.L.), the NUCLEI SciDAC program (A.L.), and the Italian National Institute for Nuclear Research (INFN), under grant TEONGRAV (O.B. and L.T.).

Data Availability Statement: The data supporting the conclusions of this study are available in the cited literature and within the present article.

Conflicts of Interest: The authors declare no conflict of interest.

References

1. Baiotti, L.; Rezzolla, L. Binary neutron star mergers: a review of Einstein’s richest laboratory. *Rep. Prog. in Phys.* **2017**, *80*, 096901. <https://doi.org/10.1088/1361-6633/aa67bb>.
2. Raithel, C.A.; Paschalidis, V.; Özel, F. Realistic finite-temperature effects in neutron star merger simulations. *Phys. Rev. D* **2021**, *104*, 063016. <https://doi.org/10.1103/PhysRevD.104.063016>.
3. Figura, A.; Lu, J.J.; Burgio, G.F.; Li, Z.H.; Schulze, H.J. Hybrid equation of state approach in binary neutron-star merger simulations. *Phys. Rev. D* **2020**, *102*, 043006. <https://doi.org/10.1103/PhysRevD.102.043006>.
4. Figura, A.; Li, F.; Lu, J.J.; Burgio, G.F.; Li, Z.H.; Schulze, H.J. Binary neutron star merger simulations with hot microscopic equations of state. *Phys. Rev. D* **2021**, *103*, 083012. <https://doi.org/10.1103/PhysRevD.103.083012>.
5. Hammond, P.; Hawke, I.; Andersson, N. Thermal aspects of neutron star mergers. *Phys. Rev. D* **2021**, *104*, 103006. <https://doi.org/10.1103/PhysRevD.104.103006>.
6. Alford, M.G.; Bovard, L.; Hanauske, M.; Rezzolla, L.; Schwenzer, K. Viscous Dissipation and Heat Conduction in Binary Neutron-Star Mergers. *Phys. Rev. Lett.* **2018**, *120*, 041101. <https://doi.org/10.1103/PhysRevLett.120.041101>.
7. Camelió, G.; Lovato, A.; Gualtieri, L.; Benhar, O.; Pons, J.A.; Ferrari, V. Evolution of a proto-neutron star with a nuclear many-body equation of state: Neutrino luminosity and gravitational wave frequencies. *Phys. Rev. D* **2017**, *96*, 043015. <https://doi.org/10.1103/PhysRevD.96.043015>.
8. Prakash, M.; Bombaci, I.; Prakash, M.; Ellis, P.J.; Lattimer, J.M.; Knorren, R. Composition and structure of protoneutron stars. *Physics Reports* **1997**, *280*, 1–77. [https://doi.org/10.1016/S0370-1573\(96\)00023-3](https://doi.org/10.1016/S0370-1573(96)00023-3).
9. Kaplan, J.D.; Ott, C.D.; O’Connor, E.P.; Kiuchi, K.; Roberts, L.; Duez, M. The influence of thermal pressure on equilibrium models of hypermassive neutron star merger remnants. *The Astrophysical Journal* **2014**, *790*, 19. <https://doi.org/10.1088/0004-637X/790/1/19>.
10. Lu, J.J.; Li, Z.H.; Burgio, G.F.; Figura, A.; Schulze, H.J. Hot neutron stars with microscopic equations of state. *Phys. Rev. C* **2019**, *100*, 054335. <https://doi.org/10.1103/PhysRevC.100.054335>.
11. Kanzawa, H.; Oyamatsu, K.; Sumiyoshi, K.; Takano, M. Variational calculation for the equation of state of nuclear matter at finite temperatures. *Nucl. Phys. A* **2007**, *791*, 232. <https://doi.org/10.1016/j.nuclphysa.2007.01.098>.
12. Benhar, O.; Lovato, A. Perturbation theory of nuclear matter with a microscopic effective interaction. *Phys. Rev. C* **2017**, *96*, 054301. <https://doi.org/10.1103/PhysRevC.96.054301>.
13. Benhar, O.; Lovato, A.; Camelió, G. Modeling Neutron Star Matter in the Age of Multimessenger Astrophysics. *The Astrophysical Journal* **2022**, *959*, 52. <https://doi.org/10.3847/1538-4357/ac8e61>.
14. Tonetto, L.; Benhar, O. Thermal effects on nuclear matter properties. *Phys. Rev. D* **2022**, *106*, 103020. <https://doi.org/10.1103/PhysRevD.106.103020>.
15. Wiringa, R.B.; Stoks, V.G.J.; Schiavilla, R. An Accurate nucleon-nucleon potential with charge independence breaking. *Phys. Rev. C* **1995**, *51*, 38–51. <https://doi.org/10.1103/PhysRevC.51.38>.
16. Carlson, J.; Pandharipande, V.R.; Wiringa, R.B. Three-nucleon interaction in 3-, 4- and ∞ -body systems. *Nucl. Phys. A* **1983**, *401*, 59. [https://doi.org/10.1016/0375-9474\(83\)90336-6](https://doi.org/10.1016/0375-9474(83)90336-6).

17. Pudliner, B.S.; Pandharipande, V.R.; Carlson, J.; Wiringa, R.B. Quantum Monte Carlo calculations of $A \leq 6$ nuclei. *Phys. Rev. Lett.* **1995**, *74*, 4396. <https://doi.org/10.1103/PhysRevLett.74.4396>.
18. Carlson, J.; Gandolfi, S.; Pederiva, F.; Pieper, S.C.; Schiavilla, R.; Schmidt, K.E.; Wiringa, R.B. Quantum Monte Carlo methods for nuclear physics. *Rev. Mod. Phys.* **2015**, *87*, 1067. <https://doi.org/10.1103/RevModPhys.87.1067>.
19. Clark, J.W. Variational theory of nuclear matter. *Prog. Part. Nucl. Phys.* **1979**, *2*, 89. [https://doi.org/10.1016/0146-6410\(79\)90004-8](https://doi.org/10.1016/0146-6410(79)90004-8).
20. Fantoni, S.; Fabrocini, A. Correlated Basis Function Theory for Fermion Systems. In *Microscopic Quantum Many-Body Theories and Their Applications*; Jesús Navarro and Artur Polls., Ed.; Springer, Berlin, Heidelberg, 1998; Vol. 501, *Lecture Notes in Physics*, p. 119. <https://doi.org/https://doi.org/10.1007/BFb0104526>.
21. Cowell, S.; Pandharipande, V.R. Quenching of weak interactions in nucleon matter. *Phys. Rev. C* **2003**, *67*, 035504. <https://doi.org/10.1103/PhysRevC.67.035504>.
22. Cowell, S.T.; Pandharipande, V.R. Neutrino mean free paths in cold symmetric nuclear matter. *Phys. Rev.* **2004**, *C70*, 035801. <https://doi.org/10.1103/PhysRevC.70.035801>.
23. Benhar, O.; Valli, M. Shear viscosity of neutron matter from realistic nucleon-nucleon interactions. *Phys. Rev. Lett.* **2007**, *99*, 232501. <https://doi.org/10.1103/PhysRevLett.99.232501>.
24. Lovato, A.; Losa, C.; Benhar, O. Weak response of cold symmetric nuclear matter at three-body cluster level. *Nucl. Phys. A* **2013**, *901*, 22. <https://doi.org/10.1016/j.nuclphysa.2013.01.029>.
25. Lovato, A.; Benhar, O.; Gandolfi, S.; Losa, C. Neutral-current interactions of low-energy neutrinos in dense neutron matter. *Phys. Rev.* **2014**, *C89*, 025804. <https://doi.org/10.1103/PhysRevC.89.025804>.
26. Wiringa, R.B.; Pieper, S.C. Evolution of nuclear spectra with nuclear forces. *Phys. Rev. Lett.* **2002**, *89*, 182501. <https://doi.org/10.1103/PhysRevLett.89.182501>.
27. Fujita, J.; Miyazawa, H. Pion Theory of Three-Body Forces. *Prog. Theor. Phys.* **1957**, *17*, 360. <https://doi.org/10.1143/PTP.17.360>.
28. Lovato, A.; Bombaci, I.; Logoteta, D.; Piarulli, M.; Wiringa, R.B. Benchmark calculations of infinite neutron matter with realistic two- and three-nucleon potentials. *Phys. Rev. C* **2022**, *105*, 055808. <https://doi.org/10.1103/PhysRevC.105.055808>.
29. Akmal, A.; Pandharipande, V.R.; Ravenhall, D.G. Equation of state of nucleon matter and neutron star structure. *Phys. Rev. C* **1998**, *58*, 1804. <https://doi.org/10.1103/PhysRevC.58.1804>.
30. Thouless, D. *The Quantum Mechanics of Many-Body Systems*; Academic Press, New York, 1961.
31. Landau, L.D.; Lifshitz, E.M. *Statistical Physics*; Pergamon Press, Oxford, 1969.
32. Baldo, M., Ed. *Nuclear Matter and the Nuclear Equation of State*; World Scientific, Singapore, 1990.
33. Hugenholtz, N.M.; Van Hove, L. A theorem on the single particle energy in a Fermi gas with interaction. *Physica* **1958**, *24*, 363. [https://doi.org/https://doi.org/10.1016/S0031-8914\(58\)95281-9](https://doi.org/https://doi.org/10.1016/S0031-8914(58)95281-9).
34. Lejeune, A.; Grange, P.; Martzoff, M.; Cugnon, J. Hot nuclear matter in an extended Brueckner approach. *Nucl. Phys. A* **1986**, *453*, 189. [https://doi.org/https://doi.org/10.1016/0375-9474\(86\)90010-2](https://doi.org/https://doi.org/10.1016/0375-9474(86)90010-2).
35. Heyer, J.; Kuo, T.T.S.; Shen, J.P.; Wu, S.S. Finite-temperature density-dependent HF calculation of nuclear matter with Gogny interaction. *Phys. Lett. B* **1988**, *202*, 465. [https://doi.org/https://doi.org/10.1016/0370-2693\(88\)91844-8](https://doi.org/https://doi.org/10.1016/0370-2693(88)91844-8).
36. Chandrasekhar, S. Solutions of Two Problems in the Theory of Gravitational Radiation. *Phys. Rev. Lett.* **1970**, *24*, 611. <https://doi.org/10.1103/PhysRevLett.24.611>.
37. Chandrasekhar, S. The Effect of gravitational radiation on the secular stability of the Maclaurin spheroid. *The Astrophysical Journal* **1970**, *161*, 561. <https://doi.org/10.1086/150560>.
38. Friedman, J.L.; Schutz, B.F. Secular instability of rotating Newtonian stars. *The Astrophysical Journal* **1978**, *222*, 281. <https://doi.org/10.1086/156143>.
39. Andersson, N.; Kokkotas, K.D. The r-mode instability in rotating neutron stars. *Int. J. Mod. Phys. D* **2001**, *10*, 381. <https://doi.org/https://doi.org/10.1142/S0218271801001062>.
40. B.P. Abbott *et al.* (LIGO Scientific Collaboration and Virgo Collaboration). GW170817: Observation of Gravitational Waves from a Binary Neutron Star Inspiral. *Phys. Rev. Lett.* **2017**, *119*, 161101. <https://doi.org/doi.org/10.1103/PhysRevLett.119.161101>.
41. Alford, M.G.; Harris, S.P. Damping of density oscillations in neutrino-transparent nuclear matter. *Phys. Rev. C* **2019**, *100*, 035803. <https://doi.org/10.1103/PhysRevC.100.035803>.
42. Landau, L.D.; Lifshitz, E.M. *Fluid Mechanics, 2nd edition*; Butterworth-Heinemann, Oxford, 1987.
43. Schaefer, T. Fluid Dynamics and Viscosity in Strongly Correlated Fluids. *Ann. Rev. Nucl. Part. Sci.* **2014**, *64*, 125. <https://doi.org/10.1146/annurev-nucl-102313-025439>.
44. Haensel, P.; Schaeffer, R. Bulk viscosity of hot-neutron-star matter from direct URCA processes. *Phys. Rev. D* **1992**, *45*, 4708–4712. <https://doi.org/10.1103/PhysRevD.45.4708>.
45. Haensel, P.; Levenfish, K.P.; Yakovlev, D.G. Bulk viscosity in superfluid neutron star cores. I. direct urca processes in $npe\mu$ matter. *Astronomy & Astrophysics* **2000**, *357*, 1157. <https://doi.org/10.48550/arXiv.astro-ph/0004183>.
46. Sawyer, R.F. Bulk viscosity of hot neutron-star matter and the maximum rotation rates of neutron stars. *Phys. Rev. D* **1989**, *39*, 3804. <https://doi.org/10.1103/PhysRevD.39.3804>.
47. Benhar, O. Testing the Paradigm of Nuclear Many-Body Theory. *Particles* **2023**, *6*, 611. <https://doi.org/10.3390/particles6020035>.

Disclaimer/Publisher's Note: The statements, opinions and data contained in all publications are solely those of the individual author(s) and contributor(s) and not of MDPI and/or the editor(s). MDPI and/or the editor(s) disclaim responsibility for any injury to people or property resulting from any ideas, methods, instructions or products referred to in the content.